EVALUATING CROP BIOMASS PRODUCTIVITY AND WATER USE EFFICIENCY USING SEBAL-DERIVED EVAPOTRANSPIRATION: A CASE STUDY OF NISHON DISTRICT, KASHKADARYA REGION, UZBEKISTAN

Nozimov Doston, Zokirov Otabek

Tashkent State Transport University, Tashkent, Uzbekistan

Keywords: *Evapotranspiration; SEBAL; NDVI; Biomass; Water productivity; Landsat; Remote sensing*

ABSTRACT

This paper studies how evapotranspiration (ET) and biomass production change over time in Nishon district, Kashkadarya region, Uzbekistan, between March and October 2025. Actual daily evapotranspiration (ET24) was calculated by the SEBAL energy balance model using Landsat 8/9 satellite images at 30 m resolution. Crop biomass production was estimated with a light-use efficiency approach (Monteith model) driven by NDVI. The monthly NDVI was highest in March (0.275) and lowest in October (0.165). Biomass production followed almost the same pattern, falling from 39.3 kg/ha/day in March to a minimum of 1.0 kg/ha/day in July, then rising again to 14.5 kg/ha/day in September. The link between NDVI and biomass was strong ($R^2 = 0.87$), but the link between ET24 and biomass was weaker ($R^2 = 0.55$). A pixel-level check also found a group of pixels with very high ET24 (up to 6.6 mm/day) but almost zero biomass, which most likely come from the Tallimarjon reservoir and wet bare soil. Another small group used very little water (around 0.2 mm/day) but reached water productivity above 3.6 kg/m³. These findings show that part of the water used in the district does not turn into crop growth, and that NDVI alone gives a better picture of biomass than ET24.

1. INTRODUCTION

Evapotranspiration (ET) is one of the largest parts of the water balance in any irrigated area. In dry regions such as Kashkadarya, where most rain falls outside the growing season, almost all crop water comes from irrigation, so knowing how this water is used is important for farmers and water managers (Allen et al., 1998). However, ET by itself does not tell us how much of this water actually goes into plant growth, because evaporation also happens from bare soil, canals, and open water surfaces.

Remote sensing offers a practical way to estimate ET across large irrigated areas without many ground stations. The Surface Energy Balance Algorithm for Land (SEBAL), first developed by Bastiaanssen et al. (1998), uses satellite thermal and optical bands to solve the surface energy balance and map actual ET at field to district scale. Because of its low cost and wide spatial coverage, SEBAL has been applied in many irrigated basins of Central Asia, including the Syrdarya and Amu Darya basins of Uzbekistan (Platonov et al., 2008; Forkutsa et al., 2009).

To connect ET with crop performance, many studies combine it with vegetation indices such as the Normalized Difference Vegetation Index (NDVI, Tucker, 1979) and light-use efficiency biomass models based on the work of Monteith (1972, 1977). Bastiaanssen and Ali (2003) showed that combining SEBAL-based ET with a Monteith-type biomass model can give useful crop yield estimates, although their model worked less well for cotton than for wheat or rice. Since cotton is still a major crop in Kashkadarya region, this earlier finding is a useful point of comparison for the present study.

Although ET, NDVI, and biomass have all been studied separately in Uzbekistan, fewer studies look at how strongly these three variables relate to each other at the district scale, and how this relation can be used to find water-inefficient zones. The goal of this study is to: (1) calculate ET24 and biomass for Nishon district from March to October 2025 using Landsat 8/9 and the SEBAL model, (2) test the statistical relationship between ET24, NDVI and biomass, and (3) classify field zones by water productivity to identify possible water losses.

2. STUDY AREA AND DATA

Nishon district is located in the western part of Kashkadarya region, in southern Uzbekistan. The district covers about 2,110 km² and has a population of around 155,500. The local climate is dry and continental, with hot summers and cold winters, and irrigation depends mostly on canal water from the Kashkadarya river system. The Tallimarjon reservoir, a large water body, is located inside the district and is visible in the satellite images used in this study as a stable area of very low NDVI and high evaporation.

The analysis used Landsat 8/9 Collection 2 Level-2 surface reflectance and surface temperature products at 30 m resolution. Cloud-free scenes covering the district were collected for eight months, from March to October 2025, with one representative scene processed for each month. For each scene, NDVI was calculated from the red and near-infrared bands, and the SEBAL model was used to calculate daily actual evapotranspiration (ET24). Biomass production (kg/ha/day) was estimated for the same scenes using a light-use efficiency model driven by NDVI.

3. METHODS

3.1 NDVI Calculation

NDVI was calculated for each Landsat scene using the standard formula:

$$\mathbf{NDVI = (NIR - Red) / (NIR + Red)}$$

where NIR and Red are the surface reflectance values of the near-infrared and red bands. NDVI values range from about −1 to 1, with higher values showing denser, healthier vegetation cover, and values near zero or below showing bare soil, water, or non-vegetated surfaces.

3.2 SEBAL Evapotranspiration (ET24)

The SEBAL model (Bastiaanssen et al., 1998) solves the surface energy balance equation:

$$\mathbf{Rn = G + H + LE}$$

where Rn is net radiation, G is soil heat flux, H is sensible heat flux, and LE is latent heat flux, which is converted to instantaneous ET. Two anchor pixels, a "cold" pixel with maximum ET and a "hot" pixel with minimum or zero ET, are selected from each scene to calibrate the sensible heat flux calculation. Instantaneous ET is then extrapolated to a 24-hour value (ET24, mm/day) using the reference ET fraction method, following the standard SEBAL procedure.

3.3 Biomass Estimation

Above-ground biomass production was estimated with a light-use efficiency (LUE) approach based on the Monteith (1972, 1977) framework:

$$\mathbf{Biomass = APAR \times LUE}$$

where APAR is the absorbed photosynthetically active radiation, calculated as the product of incoming solar radiation, the fraction of PAR in total solar radiation (about 0.45–0.50), and the fraction of PAR absorbed by the canopy (fAPAR), which was estimated from NDVI using a linear relationship. LUE is the light-use efficiency coefficient (g/MJ), taken from published values for comparable semi-arid cropping systems. The model output is daily above-ground biomass production, expressed in kg/ha/day.

3.4 Water Productivity Classification

Water productivity (WP, kg/m^3) was calculated for each pixel as the ratio of biomass production to water consumption:

$$WP = Biomass / (ET24 \times 10)$$

where the factor 10 converts ET24 from mm/day to m³/ha/day. Pixels were then ranked by WP, and two extreme groups were selected for closer analysis: a "Champion" group, made of the ten pixels with the highest WP values, and an "Inefficient" group, made of pixels with zero recorded biomass despite a measurable ET24 signal.

4. RESULTS

4.1 NDVI Dynamics

The monthly NDVI maps (Figure 1) and the time series (Figure 2) show a clear decreasing trend across the study period. NDVI was highest in March (0.275) and April (0.268), dropped sharply by May (0.203), stayed almost flat between May and August (0.199–0.205), and then declined further toward October (0.165). The northern part of the district, with more diverse field patterns, kept noticeably higher NDVI values through most months compared to the southern part, where the Tallimarjon reservoir and surrounding bare land dominate the landscape.

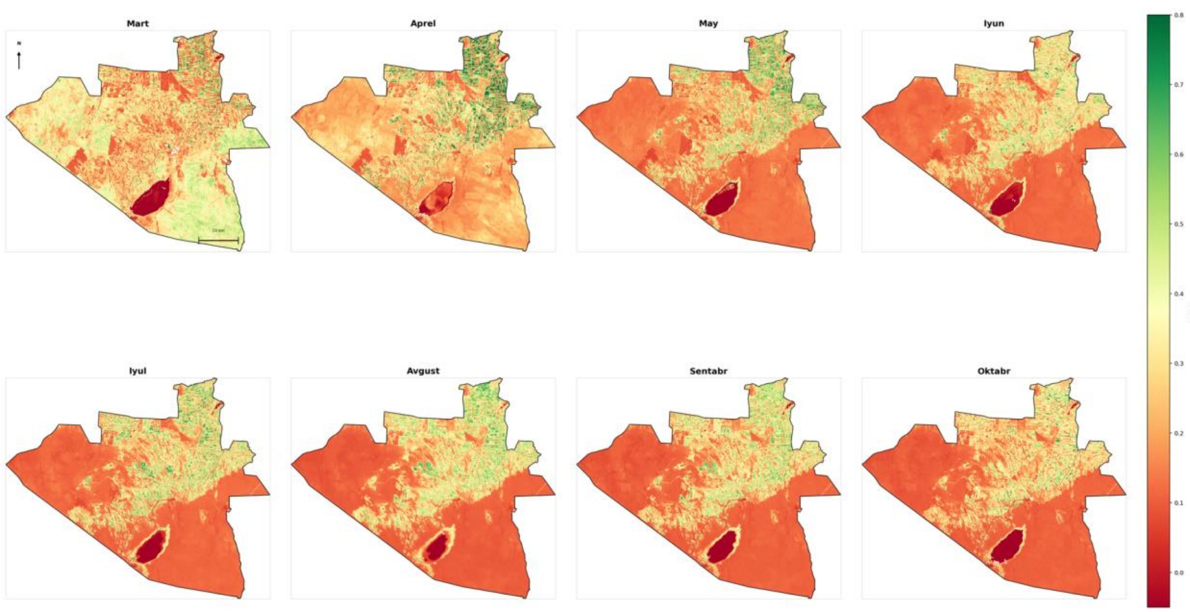

Figure 1. Monthly NDVI distribution across Nishon district, March–October 2025 (Landsat 8/9).

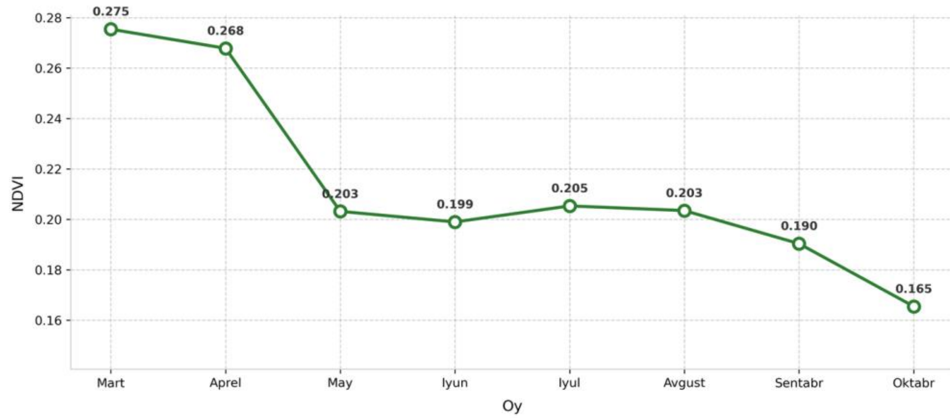

Figure 2. District-average monthly NDVI dynamics, March–October 2025.

4.2 Biomass Dynamics

Biomass production followed a similar but more extreme pattern (Figures 3 and 4). The highest district-average biomass rate was in March (39.3 kg/ha/day), falling quickly through April (24.3) and May (10.4), and reaching a clear minimum in July (1.0 kg/ha/day). After July, biomass increased again, reaching 9.1 kg/ha/day in August and a secondary peak of 14.5 kg/ha/day in September, before decreasing slightly to 11.4 kg/ha/day in October. This U-shaped pattern, with a minimum in mid-summer and a secondary peak in early autumn, differs from a typical single-peak summer crop curve, and is discussed further in Section 5.

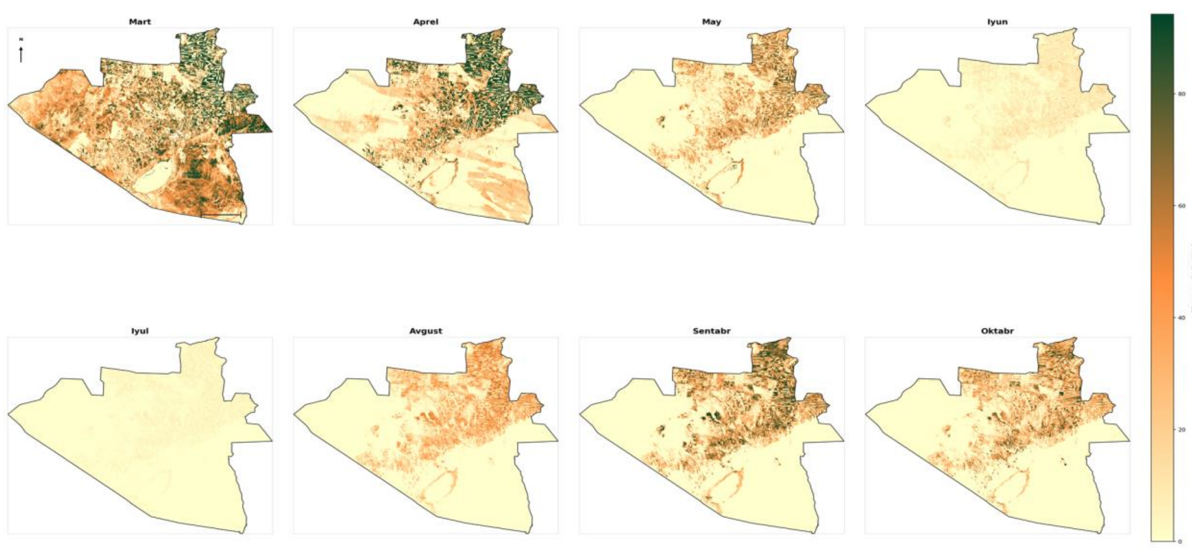

Figure 3. Monthly above-ground biomass production rate (kg/ha/day) across Nishon district, March–October 2025.

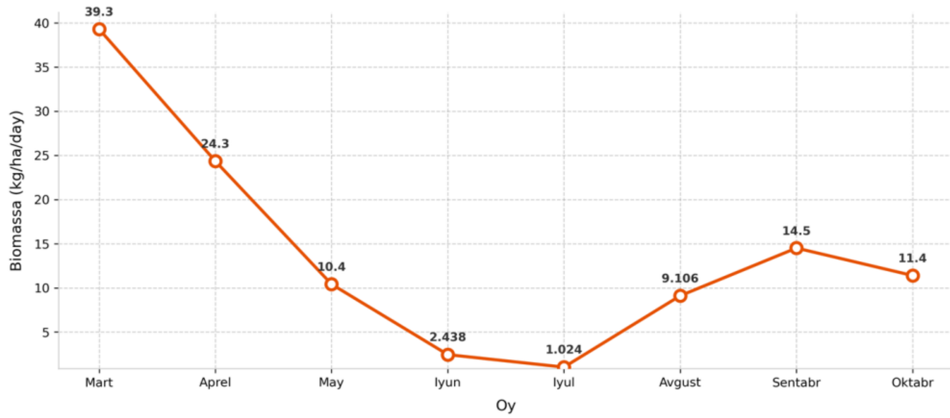

Figure 4. District-average monthly biomass production dynamics, March–October 2025.

4.3 Statistical Relationship Between ET24, NDVI and Biomass

Pixel-level scatter plots (Figures 5 and 6, Table 1) show that NDVI is a much stronger predictor of biomass than ET24 alone. The regression between NDVI and biomass gave $R^2 = 0.871$ (Biomass = 137.93 × NDVI − 16.87, $p < 0.001$), while the regression between ET24 and biomass gave only $R^2 = 0.549$ (Biomass = 7.25 × ET24 + 0.90, $p < 0.001$). Both relationships are statistically significant, but the NDVI-based one explains much more of the variation in biomass.

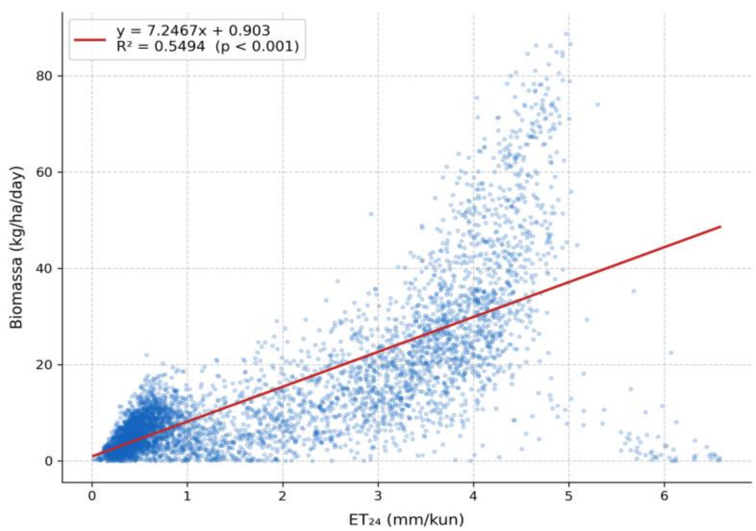

Figure 5. Relationship between ET24 and biomass production rate (pixel-level, all months).

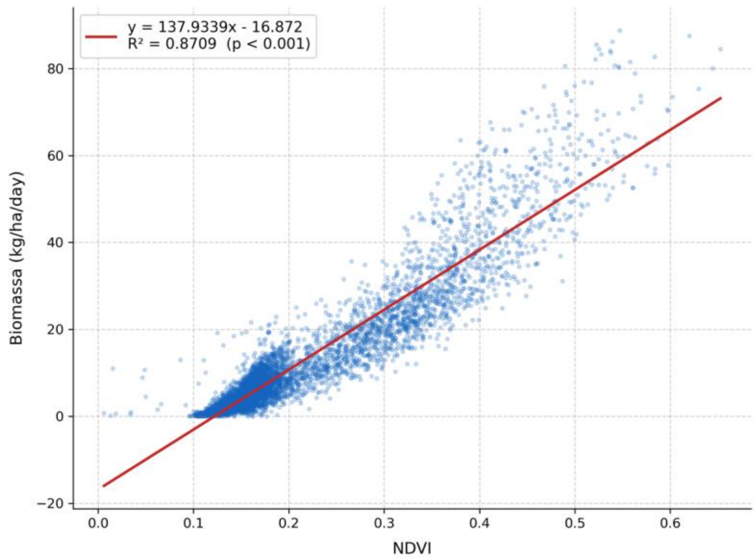

Figure 6. Relationship between NDVI and biomass production rate (pixel-level, all months).

Table 1. Coefficient of Determination (R^2) for Biomass Predictors

Relationship	R^2	Interpretation
NDVI ↔ Biomass	0.871	Strong; vegetation index directly reflects canopy growth
ET_{24} ↔ Biomass	0.549	Moderate; ET includes non-productive evaporation losses

4.4 Water Productivity Zones

Table 2 compares the "Champion" and "Inefficient" pixel groups defined in Section 3.4. Champion pixels used very little water, on average 0.21 mm/day, but still produced an average of 7.74 kg/ha/day of biomass, giving a high average water productivity of 3.70 kg/m³. In contrast, Inefficient pixels had a much higher average ET24 of 3.56 mm/day (up to 6.6 mm/day) but produced no measurable biomass, so their water productivity was effectively zero. These pixels are located mostly around the Tallimarjon reservoir shoreline and in low-lying wet areas, where evaporation happens from open water or saturated bare soil rather than from crop canopy.

Table 2. Comparison of Champion and Inefficient Pixel Groups (n = 10 each)

Group	ET_{24} mean (range), mm/day	Biomass mean, kg/ha/day	WP mean, kg/m³
Champion (Top 10 WP)	0.21 (0.03–0.26)	7.74	3.70
Inefficient (Bottom 10, zero biomass)	3.56 (0.18–6.60)	0.00	0.00

5. DISCUSSION

The U-shaped seasonal pattern of NDVI and biomass, with the lowest values around June-July and a recovery toward September, most likely reflects the local cropping calendar rather than a problem in the model. In Kashkadarya region, winter wheat is normally harvested in June, leaving bare stubble fields with very low NDVI for several weeks. At the same time, cotton, the dominant summer crop in the district, is usually still building its canopy in June-July and does not reach full ground cover until later in summer. The combination of these two effects, post-harvest wheat fields and a not-yet-closed cotton canopy, can explain why the district-average NDVI and biomass reach their lowest point exactly in this period, before cotton canopy growth and any late-summer crops push the average back up in August-September. The October decrease is consistent with cotton defoliation and harvest preparation.

The much stronger relationship between NDVI and biomass (R^2 = 0.87) compared to ET24 and biomass (R^2 = 0.55) fits well with the physical meaning of each variable. NDVI reacts directly to the amount and health of green leaf area, so it is closely tied to the photosynthetic capacity that drives biomass growth. ET24, however, mixes together plant transpiration with evaporation from bare soil, wet field edges, canals, and the Tallimarjon reservoir; none of this non-plant evaporation adds to biomass, which weakens the ET-biomass relationship at the district scale. This matches the earlier finding of Bastiaanssen and Ali (2003), who reported that Monteith-type biomass models combined with SEBAL performed less well for cotton than for wheat or rice, partly because cotton fields in their study area also showed a more complex mix of soil and canopy signals during the growing season.

The comparison between Champion and Inefficient pixel groups (Table 2) gives a practical illustration of the difference between beneficial and non-beneficial water use, a concept widely used in irrigation performance and water accounting studies (Molden, 1997; Platonov et al., 2008). Champion pixels combine low ET24 with measurable biomass, suggesting either efficient drip or furrow irrigation, or simply small, well-managed plots where most of the consumed water supports plant growth. Inefficient pixels, on the other hand, show high ET24 with no biomass at all, which is the typical signature of open water evaporation or saturated bare soil rather than crop water use. Because these pixels sit mainly along the Tallimarjon reservoir and in low drainage areas, their high water loss is expected and not necessarily a sign of poor farm management, but it is still useful information for district-level water accounting, especially under current national efforts to improve irrigation water efficiency.

Some limitations should be mentioned. The biomass model used here is empirical and was not checked against field-measured yield or biomass data for Nishon district, so the absolute biomass values should be treated with caution; the relative seasonal pattern and the relationship with NDVI are likely more reliable than the exact numbers. Also, only one Landsat scene per month was used, so short-term changes between scenes, such as a sudden irrigation event or a rain shower, are not captured. Future work could add field-based biomass or yield sampling, use a higher-frequency satellite source such as Sentinel-2, and separate cotton fields from wheat fields and water bodies before calculating district averages, to remove the mixing effect described above.

6. CONCLUSION

This study used Landsat 8/9 imagery and the SEBAL model to estimate evapotranspiration and biomass production for Nishon district, Kashkadarya region, from March to October 2025. NDVI and biomass both showed a clear seasonal pattern, with the highest values in early spring, a minimum around June-July, and a partial recovery in September, a pattern that fits the local wheat-cotton cropping calendar. NDVI was found to be a much stronger predictor of biomass ($R^2 = 0.87$) than ET24 alone ($R^2 = 0.55$), because ET24 includes evaporation from non-vegetated surfaces such as the Tallimarjon reservoir and wet bare soil. Pixel-level analysis identified clear "Champion" zones with low water use and high biomass output, and "Inefficient" zones with high water loss and no biomass, showing that simple ET-biomass mapping can help identify where irrigation water is not being used for crop production. This kind of low-cost, satellite-based approach can support more detailed water accounting and irrigation planning in Kashkadarya region and in other irrigated districts of Uzbekistan with similar conditions.

REFERENCES

Allen, R.G., Pereira, L.S., Raes, D., & Smith, M. (1998). Crop evapotranspiration — Guidelines for computing crop water requirements. FAO Irrigation and Drainage Paper No. 56. Food and Agriculture Organization of the United Nations, Rome.

Bastiaanssen, W.G.M., Menenti, M., Feddes, R.A., & Holtslag, A.A.M. (1998). A remote sensing surface energy balance algorithm for land (SEBAL): 1. Formulation. Journal of Hydrology, 212–213, 198–212.

Bastiaanssen, W.G.M., & Ali, S. (2003). A new crop yield forecasting model based on satellite measurements applied across the Indus Basin, Pakistan. Agriculture, Ecosystems & Environment, 94(3), 321–340.

Forkutsa, I., Sommer, R., Shirokova, Y.I., Lamers, J.P.A., Kienzler, K., Tischbein, B., Martius, C., & Vlek, P.L.G. (2009). Modeling irrigated cotton with shallow groundwater in the Aral Sea Basin of Uzbekistan: II. Soil salinity dynamics. Irrigation Science, 27(4), 319–330.

Gorelick, N., Hancher, M., Dixon, M., Ilyushchenko, S., Thau, D., & Moore, R. (2017). Google Earth Engine: Planetary-scale geospatial analysis for everyone. Remote Sensing of Environment, 202, 18–27.

Molden, D. (1997). Accounting for Water Use and Productivity. SWIM Paper 1. International Irrigation Management Institute, Colombo, Sri Lanka.

Monteith, J.L. (1972). Solar radiation and productivity in tropical ecosystems. Journal of Applied Ecology, 9(3), 747–766.

Monteith, J.L. (1977). Climate and the efficiency of crop production in Britain. Philosophical Transactions of the Royal Society of London B, 281(980), 277–294.

Platonov, A., Thenkabail, P.S., Biradar, C.M., Cai, X., Gumma, M., Dheeravath, V., Cohen, Y., Alchanatis, V., Goldshlager, N., Ben-Dor, E., Vithanage, J., Manthrithilake, H., Kendjabaev, S., & Isaev, S. (2008). Water productivity mapping (WPM) using Landsat ETM+ data for the irrigated croplands of the Syrdarya River Basin in Central Asia. Sensors, 8(12), 8156–8180.

Senay, G.B., Bohms, S., Singh, R.K., Gowda, P.H., Velpuri, N.M., Alemu, H., & Verdin, J.P. (2013). Operational evapotranspiration mapping using remote sensing and weather datasets: A new parameterization for the SSEB approach. JAWRA Journal of the American Water Resources Association, 49(3), 577–592.

Tucker, C.J. (1979). Red and photographic infrared linear combinations for monitoring vegetation. Remote Sensing of Environment, 8(2), 127–150.